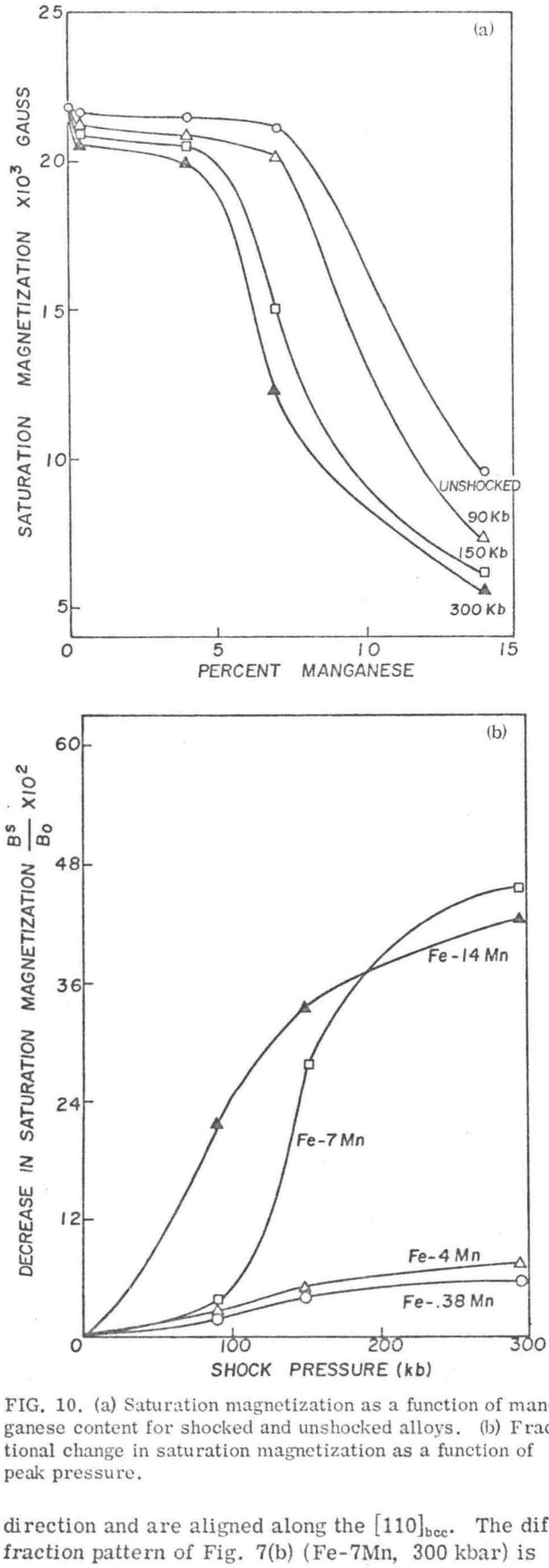

FIG. 10. (a) Saturation magnetization as a function of manganese content for shocked and unshocked alloys. (b) Fractional change in saturation magnetization as a function of peak pressure.

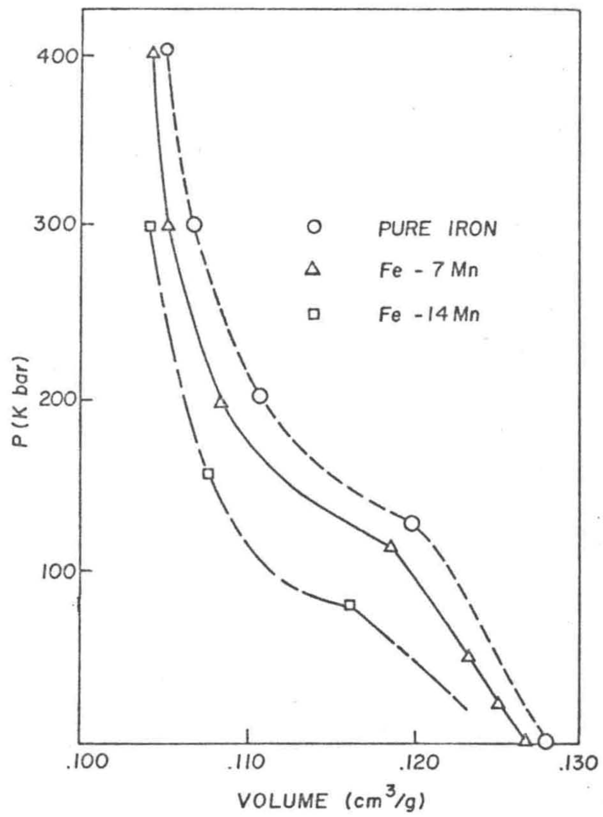

FIG. 11. Hugoniot curves for Fe–Mn alloys.

direction and are aligned along the $[110]_{bcc}$. The diffraction pattern of Fig. 7(b) (Fe-7Mn, 300 kbar) is primarily fcc; and, when the bcc and fcc diffraction patterns are superimposed, the following crystallographic relationship was obtained:

$$[\bar{1}11]_\gamma \| [110]_m, \quad (101)_\gamma \| (\bar{1}1\bar{1})_m. \tag{1}$$

This orientation relationship corresponds to that of Kurdjumov and Sachs.

The habit plane of the fcc phase in shocked Fe-7Mn was determined by single surface trace analysis. Two different types of habit planes were observed at 90 kbar. Five habits were approximately $(\bar{1}\bar{1}2)_\gamma$ and only one was near $(\overline{22}5)_\gamma$. At 150 kbar, for the variant of the orientation relationship used, the habit plane was always found to be near $(\bar{1}\bar{1}2)_\gamma$.

D. Magnetization Measurements

The magnetization curves appearing in Fig. 9 indicate different approaches to saturation at each pressure. In general there is a lowering of saturation magnetization with increasing shock pressure, as shown in Fig. 10(a). The fractional decrease in saturation magnetization is shown in Fig. 10(b). The greatest fractional change in saturation magnetization occurred for the Fe-7Mn alloy, which was shocked at 300 kbar. However, at 150 kbar the change in saturation magnetization was greater for the Fe-14Mn than for the Fe-7Mn alloy. This observation is consistent with the density measurements. Figure 10(a) shows that the saturation magnetization changes only slightly with shock pressure when the manganese content is below 4 wt%. This means that the change in the B-H curve produced by dislocations is relatively small compared to the change produced